INSTITUTE OF PHYSICS PUBLISHING JOURNAL OF PHYSICS B: ATOMIC, MOLECULAR AND OPTICAL PHYSICS

J. Phys. B: At. Mol. Opt. Phys. **38** (2005) 4363–4378 doi:10.1088/0953-4075/38/24/003

Cross sections for electron-impact excitation of the H_2 molecule using the MOB-SCI strategy

Romarly F da Costa, Fernando J da Paixão and Marco A P Lima

Instituto de Física 'Gleb Wataghin', Universidade Estadual de Campinas, Caixa Postal 6165, 13083-970, Campinas, São Paulo, Brazil

Received 26 August 2005, in final form 30 October 2005
Published 28 November 2005
Online at stacks.iop.org/JPhysB/38/4363

Abstract

In this paper, we report integral and differential cross sections for the electronic excitation of H_2 molecules by electron-impact. Our scattering amplitudes were calculated using the Schwinger multichannel method within the minimal orbital basis for single configuration interactions (MOB-SCI) level of approximation. Through the use of the present strategy we have investigated the coupling effects among ground state and first singlet and triplet states of the same spatial symmetry. The five-state (nine for degenerated states) close-coupling calculations joined the advantages of a well-described set of physical states of interest with a minimum associated pseudo-state space. The results obtained by means of the MOB-SCI technique show a significant improvement towards experimental data in comparison with previous two-channel close-coupling calculations.

1. Introduction

It has been pointed out by several authors that the electronic excitation of molecules by impact of slow electrons strongly affects the reaction dynamics in discharge environments [1–3]. For instance, detailed information concerning such inelastic process is essential for the modelling of the plasma processing gases largely used in semiconductor manufacturing. In the last few decades, the rapid growing in the number of applications of the plasma-based technologies has yielded a strident demand for the compilation of a reliable cross section database. In spite of this fact, the effort undertaken by experimentalists and theorists to generate the required data has attained just a moderate degree of success.

Due to the difficulties in producing and characterizing excited species with sufficient accuracy [4], experimental measurements on the electronic excitation by electron-impact were performed for a few molecular systems and have covered only a limited range of impact energies. Even for the simplest diatomic target, the H_2 molecule, the number of experimental results at incident energies below 50 eV is small. For this molecule, the cross section data related to low-energy electronic excitation processes were measured by Trajmar *et al* [5],

Weingartshofer *et al* [6], Watson and Anderson [7], Srivastava and Jansen [8], Hall and Andric [9], Ajello *et al* [10], Nishimura and Danjo [11], Mason and Newell [12], Khakoo and Trajmar [13–15], Khakoo and Segura [16] and, more recently, by Wrkich *et al* [17].

Theoretical calculation of accurate electronic excitation cross sections also poses a difficult task. Unlike ground state energy estimation, electron-molecule scattering does not have lower bounds, which suggests how to proceed in order to improve the accuracy of the obtained results and, as a consequence, we must learn through the analysis of performed calculations. Besides, the intrinsic many-body character of the collision problem imposes the use of approximations and this occurs at both, bound and scattering state calculations. In this way, the level of approximation employed in the description of the target states and the strategy used in the composition of the coupled-state active space are very important steps for modelling the electronic excitation processes. For instance, the use of improved virtual orbitals (IVO) [18] provides a simple and good representation of the excited states in terms of one or two Slater determinants (depending on the desired spin coupling), but leads to some limitations. Indeed, singlet and triplet IVO states could not simultaneously be taken into account in a close-coupling calculation because one of these states, constructed from the same spatial orbital, would be poorly described. So, scattering calculations in which the active space is composed by IVO states necessarily must neglect the coupling effects between distinct spin manifolds. Based on the assumption that singlet and triplet states are weakly coupled, since they only interact via exchange forces, different authors have performed their studies within the scope of the IVO approximation. Theoretical calculations done by Baluja *et al* [19] (*R*-matrix method), Schneider and Collins [20] (linear algebraic method), Lima *et al* [21, 22] and Gibson *et al* [23] (Schwinger multichannel method), Rescigno and Schneider [24] and Parker *et al* [25] (complex-Kohn method) and, finally, by Lee *et al* [26, 27] and Machado *et al* [28, 29] (continued fractions method) are examples of the utilization of this strategy in the study of the electronic excitation of H_2 molecules by impact of slow electrons. On the other hand, in the *R*-matrix calculations accomplished by Branchett *et al* [30–32] and Trevisan *et al* [33], the bound states were constructed with the use of a configuration interactions (CI) technique. These studies have enabled the investigation of competition effects among singlet and triplet states which became accessible at collision energies up to 25 eV, giving rise to the largest electron-H_2 electronic close-coupling calculations to date. A very complex CI description of the molecular target, such as those used in [30–33], leads to more flexibility in the composition of the coupled-state active space. However, it also introduces a large family of pseudo-states, which must be included in the scattering calculation in order to properly account for the flux distribution among the participant channels. A critical analysis of these sets of theoretical data points out that neither the results obtained in the above calculations nor those calculated within IVO-based close-coupling strategies provide a systematic improvement towards measured values. From this, the question which naturally arises is related to the choice of a set of competing target states to be used in the electronic close-coupling expansion. This is important because as the electron incident energy increases, a larger number of electronic states become energetically accessible. That is, all on-shell roots, physical and pseudo states, of the target Hamiltonian lying below a given collision on-shell energy must be considered as open channels. In a typical scattering calculation every channel brings complications since cross sections are very sensitive to new thresholds and, just before a threshold, an upcoming channel can give rise to resonances. Moreover, as long as pseudo-states usually have inaccurate thresholds, lots of displaced resonances would deteriorate the quality of the integrated cross sections. Apart from this fact, it is important to note that the fixed nuclei approximation fails around the threshold positions, requiring an adequate treatment of the vibrational dynamics.

From the last considerations, it is clear that the greatest problem in multichannel calculations is the restriction on the number of open channels that can be handled, even when powerful computer platforms are used. In view of the high density of nearby low-lying electronic states, for most molecules, full convergence of the close-coupling strategy is not possible away from the first excitation thresholds. Thus, it is important to develop strategies for picking up which states should be included and which should be left out in the scattering calculations. In addition, when a CI description of the target states is used, the number of associated pseudo-states must be minimized.

Having these questions in mind, we have proposed a new scheme for the study of the electron-molecule electronic excitation problem. In our modified computational codes, the excited states are constructed within a single (excitation) configuration interactions (SCI) model. In order to keep the advantages of the SCI description and also to minimize the active space of coupled-states, we have decided to use what we call the minimal orbital basis for single configuration interactions (MOB-SCI) approach. More specifically, we have chosen a minimal orbital basis that, for the first singlet and triplet states of a given symmetry representation, generates the smallest configuration space equivalent to the full single configuration one. The intention was to provide an alternative technique beyond the two-channel approach, with a minimum number of states used for the close-coupling expansion as possible. A short account of this work was recently published [34] and the preliminary differential cross section results show a very good agreement with available experimental data.

In this paper we report the complementary set of integral and differential cross sections for the electron-impact excitation of H_2 molecules. Our study includes the $X^1\Sigma_g^{(+)} \rightarrow b^3\Sigma_u^{(+)}$, $B^1\Sigma_u^{(+)}$; $X^1\Sigma_g^{(+)} \rightarrow a^3\Sigma_g^{(+)}$, $E,F^1\Sigma_g^{(+)}$; and $X^1\Sigma_g^{(+)} \rightarrow c^3\Pi_u$, $C^1\Pi_u$ electronic transitions for impact energies up to 30 eV. The scattering amplitudes were calculated using the Schwinger multichannel (SMC) method [35, 36] within the above mentioned MOB-SCI level of approximation. Through the use of the present strategy we have investigated the coupling effects among ground state and first singlet and triplet states of the same spatial symmetry. The five-state (nine for degenerated states) close-coupling calculations joined the advantages of a well-described set of physical states of interest with a minimum associated pseudo-state space. Further, an analysis of the numerical stability of present calculations is conduced through the use of a check procedure based on those developed by Chaudhuri *et al* [37, 38]. In summary, the paper is outlined as follows. In section 2 we briefly review the SMC method and describe how the MOB-SCI approach was implemented in the computational codes. More details about the numerical procedure and the discussion of the results are given in section 3. Our conclusions and perspectives are presented in section 4.

2. Theory

The Schwinger multichannel method is obtained as an extension of the original Schwinger variational principle (SVP) [39]. Details of the formulation have been given elsewhere [40, 41], and here we will only present the basic aspects of the theory. Since the SVP is a variational method for the scattering amplitude, the total scattering wave function can be expanded in a trial basis set,

$$\left|\Psi_{\vec{k}}^{(\pm)}\right\rangle = \sum_m a_m^{(\pm)}(\vec{k})|\chi_m\rangle; \tag{1}$$

and the variational determination of the coefficients $a_m^{(\pm)}(\vec{k})$ allows us to write

$$f_B^{\mathrm{SMC}}(\vec{k}_f, \vec{k}_i) = -\frac{1}{2\pi}\sum_{m,n}\left\langle S_{\vec{k}_i}\middle|V|\chi_m\right\rangle (d^{-1})_{mn}\langle\chi_n|V\left|S_{\vec{k}_f}\right\rangle, \tag{2}$$

which is the expression for the scattering amplitude in the body-frame, and where

$$d_{mn} = \langle \chi_m | A^{(+)} | \chi_n \rangle. \tag{3}$$

The program used to perform the calculations presented in this paper is a new version of the Schwinger multichannel method computer code for scattering against closed-shell targets. The formula for the $A^{(+)}$ operator was rewritten in the following way:

$$A^{(+)} = \left[PV - VG_P^{(+)}V + \hat{H}\left(\frac{1}{N+1} - P\right)\right], \tag{4}$$

whose matrix elements are, when symmetrized, equivalent to those obtained by means of the usual expression [21, 22]. In the above equations, χ_m are $(N+1)$-particle Slater determinants (just the combination needed to provide eigenstates of the global spin of the system) given by the product of a target state and a scattering function; $\vec{k}_i$ and $\vec{k}_f$ are the initial and final wave numbers of the incident and scattered electron, respectively, and V is the interaction potential. Also, $S_{\vec{k}_{i,f}}$ are products of a target wave function and a plane wave, P is a projector operator onto the open-channel space spanned by the target eigenfunctions, and $G_P^{(+)}$ is Green's function projected on the P-space. Finally, $\hat{H} \equiv E - H$, H being the total Hamiltonian and E the total energy of the system.

As can be noted from equations (2)–(4), the variational expression for the scattering amplitude contains matrix elements of the Hamiltonian operator of the system. In spite of this fact, the trial scattering wave functions do not need to satisfy any specific boundary condition, which is included in Green's function. Besides, the wave functions belonging to the configuration space always appear multiplied by the interaction potential and, therefore, must be well described only in the region where V is appreciable. This property allows an expansion of the wave functions in terms of $\mathcal{L}^2$ functions (in the present implementation we also make use of Cartesian Gaussian functions, which are especially designed for integration with multicentre reference systems). In this way, the matrix elements which appear in the expression of the scattering amplitude can analytically be computed, except those involving Green's function. The $\langle \chi_m | V G_P^{(+)} V | \chi_n \rangle$ (VGV) terms, being evaluated by numerical quadrature [41], represent the most expensive step in the calculations. Another important feature of the new SMC codes is that the scattering amplitudes are calculated in a basis where the total spin, electron plus target, is conserved [34].

As mentioned above, equation (2) provides an analytical approximation to the scattering amplitude in the body reference frame. In order to obtain cross sections which may be compared with experimental measurements, we have expanded $f_B^{\mathrm{SMC}}(\vec{k}_f, \vec{k}_i)$ in partial waves (see, for instance, [42]):

$$f_B^{\mathrm{SMC}}(\vec{k}_f, \vec{k}_i) = \sum_{\ell,m}^{\ell_{\max}} F_{\ell,m}^{\mathrm{SMC}}(k_f, \vec{k}_i) Y_\ell^m(\hat{k}_f), \tag{5}$$

with

$$F_{\ell,m}^{\mathrm{SMC}}(k_f, \vec{k}_i) = \int \mathrm{d}\hat{k}_f \, Y_\ell^{m^*}(\hat{k}_f) f_B^{\mathrm{SMC}}(\vec{k}_f, \vec{k}_i); \tag{6}$$

and performed the appropriate transformations to express the scattering amplitude in terms of the laboratory frame angles:

$$f_L^{\mathrm{SMC}}(\vec{k}'_f, \vec{k}_i) = \sum_{\ell,m,\mu}^{\ell_{\max}} F_{\ell,m}^{\mathrm{SMC}}(k_f, \vec{k}_i) Y_\ell^\mu(\hat{k}'_f) D_{m,\mu}^\ell(0, \beta, \alpha), \tag{7}$$

where $\vec{D}$ are Wigner rotation matrices whose argument consists of the Euler angles relating the two reference frames, $\hat{k}_i = (\beta, \alpha)$ and $\hat{k}'_f = (\theta', \phi')$ are the lab-frame scattering angles. The

random orientation of the target is accounted for by averaging over the incident (body-frame) angles also denoted by $\hat{k}_i$, that is,

$$\frac{d\sigma}{d\Omega}(\theta', \phi'; k_f, k_i) = \frac{1}{4\pi}\frac{k_f}{k_i}\int d\hat{k}_i \left| f_L^{SMC}(\vec{k}'_f, \vec{k}_i)\right|^2. \tag{8}$$

For a transition of interest, the physical cross sections are obtained by averaging over the azimuthal angle ϕ' and performing the appropriate average over initial and sum over final spin states.

To conclude the discussion of the theoretical aspects, it should be noted that the cross section above defined includes contributions of a finite number of angular momenta, because the partial wave decomposition is truncated at a given ℓ_{max}. Since for singlet $\rightarrow$ triplet transitions only short-range interactions of exchange nature are involved, it is usually not necessary to include a great number of partial waves to achieve the convergence of numerical integrations. Therefore, for triplet states the cross sections are obtained according to the above equations with the partial wave expansion truncated at $\ell_{max} = 2$. However, for singlet transitions the long-range character of the potential requires the use of a larger number of partial waves to properly describe the scattering in the forward direction. This can considerably enlarge the computational effort, especially for dipole-allowed transitions. To overcome such a problem the contribution from high-angular-momentum partial waves can be accounted by means of a Born-closure (BC) procedure. In this case, for angular momenta up to a given value ℓ'_{max}, contributions to the cross section were obtained from the Schwinger variational calculation, while the first Born approximation (FBA) was used to include contributions above ℓ'_{max}, that is, the term $F^{SMC}_{\ell,m}(k_f, \vec{k}_i)$ in equation (5) is replaced by

$$F^{BC}_{\ell,m}(k_f, \vec{k}_i) = \langle \ell m | f^{BC} | \vec{k}_i \rangle = \langle \ell m | f^{FBA} | \vec{k}_i \rangle + \eta \sum_{\ell' m'}^{\ell'_{max}} [\langle \ell m | f^{SMC} | \ell' m' \rangle - \langle \ell m | f^{FBA} | \ell' m' \rangle] \langle \ell' m' | \hat{k}_i \rangle \tag{9}$$

where $\eta = 0$ for $\ell > \ell'_{max}$ and $\eta = 1$ for $\ell \leqslant \ell'_{max}$. For the singlet $\rightarrow$ singlet transitions we have used $\ell'_{max} = 2$ and $\ell_{max} = 9$.

2.1. Implementation

As previously mentioned, we present in this paper the calculated cross sections obtained within the scope of the minimal orbital basis for single configuration interactions (MOB-SCI) approach. The idea is based on the fact that an excited state constructed with an IVO, calculated for a specific hole orbital, is equivalent to a complete SCI calculation out of the same hole orbital that generated the IVO. This assumption allows the construction of a pair of particle orbitals that provides a minimal configuration basis set fully equivalent to the complete SCI calculation of the chosen singlet and triplet states. In practice, the implementation of the MOB-SCI strategy was undertaken as follows. First, we have constructed a subspace composed by two orbitals, a singlet and a triplet IVOs [18] of a given target symmetry representation. These IVOs are then orthogonalized among themselves, and all virtuals orbitals are made orthogonal to them, through a usual Gram–Schmidt procedure (note that, by construction, IVOs are orthogonal to the ground state orbitals). This strategy allows the smallest expansion set of single-excitation configurations, and gives rise to two 2×2 matrices, one for the singlet and the other for the triplet Hamiltonians. The diagonalization of these matrices results in singlet and triplet states equivalent to the complete SCI calculation. The compact vector space obtained by means of the MOB-SCI technique is therefore composed by the physical excited singlet and triplet states along with a minimum set of pseudo-states.

Table 1. Cartesian Gaussian basis set, defined as $\chi_{lmn} = N_{lmn}(x - A_x)^l(y - A_y)^m(z - A_z)^n \exp(-\alpha|\vec{r} - \vec{A}|^2)$, where $\vec{A}$ locates the Gaussian center. Basis set used for the ground and excited states of the H_2 molecule, in the expansion of trial scattering wave functions, and in the insertion quadrature in the $VG_P^{(+)}V$ terms.

Centre and type	Exponent
H, 6s	48.4479, 7.283 46, 1.651 39, 0.462 447, 0.145 885, 0.07
H, 6p	4.5, 1.5, 0.5, 0.25, 0.125, 0.031 25
CM, 4s	0.25, 0.05, 0.01, 0.002
CM, 4p	0.8, 0.2, 0.0625, 0.007 81
H, 6d	4.5, 1.5, 0.5, 0.25, 0.125, 0.031 25

Table 2. Vertical excitation energy for the six lower states of the H_2 molecule in electron-volts (eV).

Estado	MOB-SCI	*R*-matrix [30]	Exact	Experimental [50]
$b^3\Sigma_u^{(+)}$	9.98	10.45	10.62 [45]	
$a^3\Sigma_g^{(+)}$	12.04	12.41	12.54 [45]	11.83
$c^3\Pi_u$	12.32	12.60	12.73 [46]	11.72
$B^1\Sigma_u^{(+)}$	12.74	13.15	12.75 [47]	11.19
$E,F^1\Sigma_g^{(+)}$	13.01	13.25	13.14 [47]	12.35
$C^1\Pi_u$	13.12	13.11	13.23 [49]	12.30

3. Results

3.1. Computational aspects

Our calculations were performed within the framework of fixed-nuclei and Frank–Condon approximations [43] at the experimental internuclear distance of 1.400 28 a_0. The wave functions of the seven lowest states of the H_2 molecule (namely, $X^1\Sigma_g^{(+)}$, $b^3\Sigma_u^{(+)}$, $a^3\Sigma_g^{(+)}$, $c^3\Pi_u$, $B^1\Sigma_u^{(+)}$, $E,F^1\Sigma_g^{(+)}$ and $C^1\Pi_u$) were expressed as a single configuration interactions representation within a minimal orbital basis, as described in section 2.1. The Cartesian Gaussian set of uncontracted functions used in the expansion of the target states and trial scattering wave functions are given in table 1. With this basis set, the calculated SCF energy at the equilibrium internuclear distance is −1.1332 au, to be compared with the Hartree–Fock limit [44] of −1.1336 au. The calculated vertical excitation energies for electronic transitions leading to the excited states considered in this work are given in table 2. For comparison we also show very accurate excitation energies obtained by *ab initio* electronic structure calculations [45–49] and the available experimental data [50]. As can be noticed, our excitation thresholds are good approximations to more sophisticated theoretical values and also to measurements.

Scattering calculations considered in this work include the ground state, first singlet and triplet states of a given symmetry representation and two pseudo-states (obtained as a result of the SCI description of the target states), giving rise to a five-state close-coupling model. For transitions involving the $c^3\Pi_u$ and $C^1\Pi_u$ degenerated states, the vector space is twice as larger and the calculations were performed with nine coupled-states. In table 3 we present, for completeness, the excitation thresholds for electronic transitions leading to all states obtained within the MOB-SCI approach.

Table 3. Vertical excitation energy for the $b^3\Sigma_u^{(+)}$ and $B^1\Sigma_u^{(+)}$; $a^3\Sigma_g^{(+)}$ and E,$F^1\Sigma_g^{(+)}$; $c^3\Pi_u$ and $C^1\Pi_u$ states of the H_2 molecule in electron-volts (eV).

State	Energy (eV)
$b^3\Sigma_u^{(+)}$	9.98
$B^1\Sigma_u^{(+)}$	12.74
Triplet pseudo-state	15.22
Singlet pseudo-state	18.98
$a^3\Sigma_g^{(+)}$	12.04
E, $F^1\Sigma_g^{(+)}$	13.01
Triplet pseudo-state	15.78
Singlet pseudo-state	18.23
$c^3\Pi_u$	12.32
$C^1\Pi_u$	13.12
Triplet pseudo-state	16.80
Singlet pseudo-state	19.37

3.2. Numerical stability analysis

It is known that in practical applications of the SMC method the evaluation of the scattering amplitudes could be affected by numerical instabilities that often work as a source of unphysical resonances. Recently, some authors have pointed out that resonances of this type can be distinguished from the physical ones and completely removed from calculated cross sections. Through the implementation of the singular value decomposition (SVD) technique in their SMC computational codes, Winstead *et al* [51] have obtained good results in the detection and control of such numerical instabilities. However, as a collateral effect of the use of the SVD method, they have to deal with an energy dependent basis set. That is, their check procedure must be applied for each considered collision on-shell energy. In order to overcome this inconvenient, Chaudhuri *et al* [37, 38] have proposed an alternative technique to study the numerical stability of the SMC calculations, in which the inspection analysis was performed for a fixed value of the impact energy. The numerical stability of present MOB-SCI calculations was investigated using a similar procedure to that developed by Chaudhuri and co-workers [37, 38]. In short, the analysis begins with the diagonalization of the matrix elements of the modified operator given by

$$\tilde{V} \equiv \frac{1}{2}(PV + VP) + \frac{1}{N+1}\left[\hat{H} - \frac{N+1}{2}(\hat{H}P + P\hat{H})\right]. \tag{10}$$

The next step consists in the identification of the configurations weakly coupled by the interaction potential, that is, the eigenvectors associated with eigenvalues of the equation $\tilde{V}|\chi_m\rangle = v_m|\chi_m\rangle$, with $v_m \approx 0$. We have removed all configurations, symmetry by symmetry, with small eigenvalues until we have obtained stable cross sections.

3.3. Results and discussion

Cross sections for the excitation of the hydrogen molecule by electron-impact involving the transitions $X^1\Sigma_g^{(+)} \rightarrow b^3\Sigma_u^{(+)}$, $B^1\Sigma_u^{(+)}$; $X^1\Sigma_g^{(+)} \rightarrow a^3\Sigma_g^{(+)}$, E,$F^1\Sigma_g^{(+)}$; and $X^1\Sigma_g^{(+)} \rightarrow c^3\Pi_u$, $C^1\Pi_u$ states are reported in the energy range from excitation thresholds up to 30 eV.

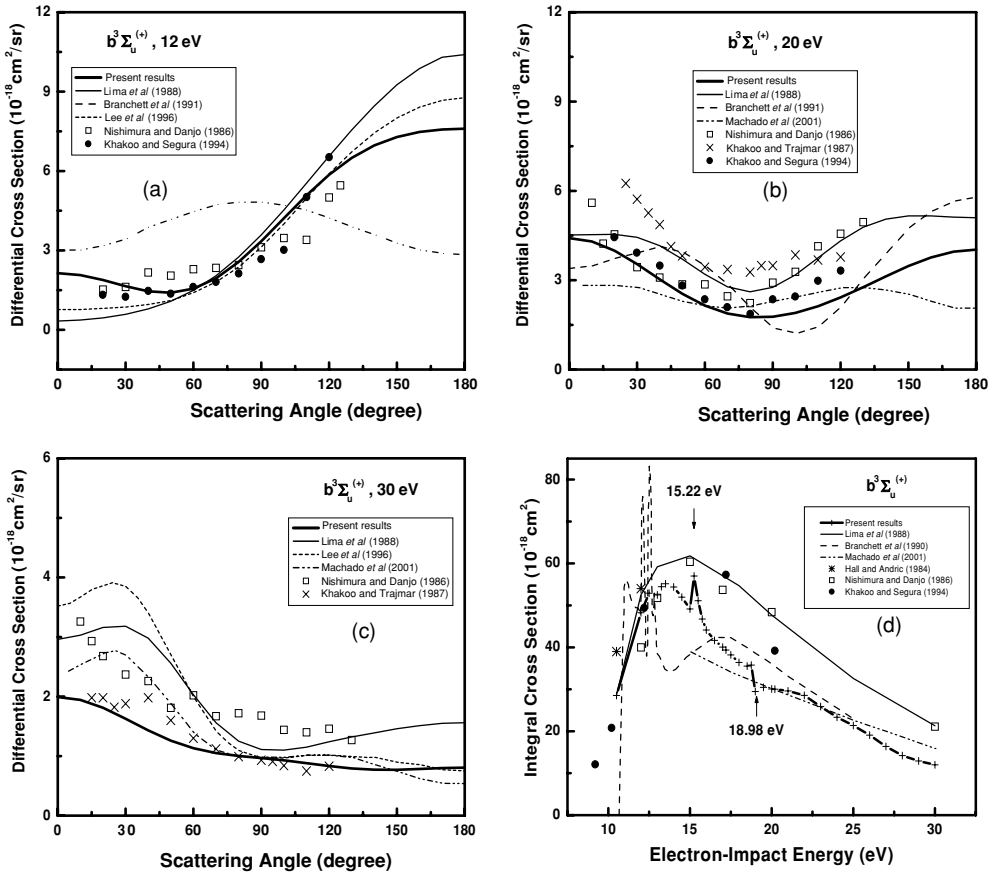

Figure 1. Differential and integral cross sections for the $X^1\Sigma_g^{(+)} \rightarrow b^3\Sigma_u^{(+)}$ electronic transition of the H_2 molecule: (a) DCS at 12 eV, (b) DCS at 20 eV, (c) DCS at 30 eV and (d) ICS. Thick solid line: present results; solid line: SMC two-state results from Lima *et al* [22]; dashed line: *R*-matrix seven-state results from Branchett *et al* [32]; short dashed line: continued fractions two-state results from Lee *et al* [26]; dash-dot-dotted line: continued fractions four-state results from Machado *et al* [28]; stars, open squares, crosses and full circles: experimental results from Hall and Andric [9], Nishimura and Danjo [11], Khakoo and Trajmar [15] and Khakoo and Segura [16], respectively.

3.3.1. The $X^1\Sigma_g^{(+)} \rightarrow b^3\Sigma_u^{(+)}$ *electronic transition.* In figures 1(a)–(c) we present the differential cross sections (DCS) for the electronic excitation from ground state to the $b^3\Sigma_u^{(+)}$ state at the incident energies of 12, 20 and 30 eV. The agreement between MOB-SCI results and available experimental data is, in general, very good. Particularly, we note that at the energies of 12 and 20 eV our DCS reproduce the small angle behaviour observed in the measurements from Nishimura and Danjo [11] and Khakoo and Segura [16]. These results clearly denote an improvement on previous two-channel calculations from Lima *et al* [22] (SMC) and Lee *et al* [26] (MCF), and also on the strong close-coupling calculations from Branchett *et al* [32] (*R*-matrix) and Machado *et al* [28] (MCF). Although not shown, at 13 eV there is a similar agreement between the MOB-SCI differential cross section and measured values from [11]. For the incident energy of 30 eV, our DCS is better compared to the experimental data from Khakoo and Trajmar [13] and lies systematically below the theoretical results from Lima *et al*

[22] (SMC). The DCS also lies below the results obtained by Lee *et al* [26] and Machado *et al* [28] (MCF), except for angles above 150°, where our result is a little bit more backward peaked. Figure 1(d) shows the integral cross section (ICS) for the $X^1\Sigma_g^{(+)} \rightarrow b^3\Sigma_u^{(+)}$ electronic transition. In the energy range up to 15 eV, the MOB-SCI result is in good agreement with the measurements from Hall and Andric [9], Nishimura and Danjo [11] and Khakoo and Segura [16]. Above this energy our result is smaller than experimental data, but compares very well with the four-state calculation from Machado *et al* [28] (MCF) and the six-state calculation from Branchett *et al* [31]. The disagreement between MOB-SCI and early two-channel ICS results from Lima *et al* [22] (SMC) at energies above 15 eV is not surprising. In fact, at this energy the present calculation includes other energetically accessible states in the close-coupling expansion and hence allows for the flux, giving rise to the reduction in the ICS magnitude. Finally, we notice the appearance of three resonant structures in the MOB-SCI integral cross section, which are related to the threshold phenomena of the upcoming channels (first $^1\Sigma_u^{(+)}$, and second $^3\Sigma_u^{(+)}$ and $^1\Sigma_u^{(+)}$ states, as indicated in table 3) present in our five-state close-coupling calculation.

3.3.2. The $X^1\Sigma_g^{(+)} \rightarrow B^1\Sigma_u^{(+)}$ electronic transition. Figures 2(a)–(c) show our DCS results for the $X^1\Sigma_g^{(+)} \rightarrow B^1\Sigma_u^{(+)}$ transition at the incident energies of 17.5, 20 and 30 eV along with the measurements from Srivastava and Jansen [8], Khakoo and Trajmar [14], Wrkich *et al* [17] and also, the calculations from Gibson *et al* [23] (SMC), Branchett *et al* [32] (*R*-matrix) and Machado *et al* [28] (MCF). The small angle DCS behaviour is dominated by the long-range dipole contribution, included in our calculations through a Born-closure procedure [23], as discussed before. The overall agreement between MOB-SCI results and calculated and measured cross sections is quite good, especially in the angular region above 30°. As could be seen in figure 2(d), our integral cross section (ICS) also compares well with available experimental data. In spite of the good agreement of the DCS result at the incident energy of 30 eV, it is worthwhile to note that the MOB-SCI calculation provides an ICS around 50% higher in magnitude. The errors introduced in the extrapolation procedure used to derive the experimental cross section may explain the great discrepancy observed at this energy. With respect to the theoretical calculations from [32] (*R*-matrix) and [28] (MCF), our results reproduce the ICS energy dependence in shape, but not in magnitude. The differences are possibly related to the strategy used in the composition of the active space of coupled states. A small resonance, associated with the threshold position of the second $^1\Sigma_u^{(+)}$ pseudo-state, could also be observed.

3.3.3. The $X^1\Sigma_g^{(+)} \rightarrow a^3\Sigma_g^{(+)}$ electronic transition. In figures 3(a)–(c) we show the differential cross sections for the transition from ground state to the $a^3\Sigma_g^{(+)}$ electronic state. Our DCS at the incident energies of 15, 20 and 30 eV are compared with those from Lima *et al* [22] (SMC), Branchett *et al* (*R*-matrix) [31], Parker *et al* (complex-Kohn) [25] and Machado *et al* (MCF) [28]. The experimental data from Khakoo and Trajmar [13] and Wrkich *et al* [17] are also included. The agreement among the cross sections calculated by means of different theoretical approaches is, in general, far from satisfactory. At 15 eV the MOB-SCI results are smaller than those obtained in the calculation from Lima *et al* [22] (SMC) in the whole angular interval. Once again we note that the DCS obtained in the two-state approach would be overestimated, since the coupling effects due to higher accessible electronic states are neglected. The absence of measured values at this energy prevents a more detailed discussion. For the incident energy of 20 eV the agreement with the measurements from Khakoo and Trajmar [13] and Wrkich *et al* [17] is good, although for angles below 60°, and the MOB-SCI cross section is slightly less

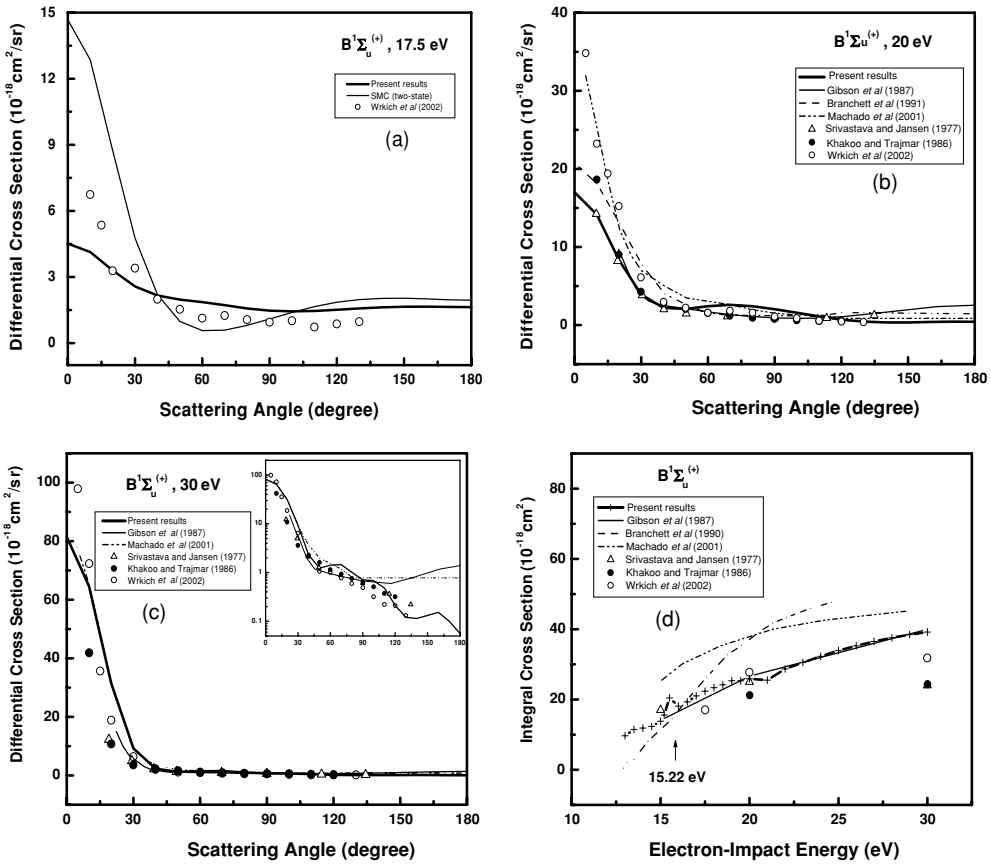

Figure 2. Differential and integral cross sections for the $X^1\Sigma_g^{(+)} \rightarrow B^1\Sigma_u^{(+)}$ electronic transition of the H_2 molecule: (a) DCS at 17.5 eV, (b) DCS at 20 eV, (c) DCS at 30 eV and (d) ICS. Thick solid line: present results; solid line: SMC two-state results from Gibson *et al* [23]; dashed line: *R*-matrix seven-state results from Branchett *et al* [31, 32]; dash-dot-dotted line: continued fractions four-state results from Machado *et al* [29]; open triangles, full circles and open circles: experimental results from Srivastava and Jansen [8], Khakoo and Trajmar [14] and Wrkich *et al* [17], respectively.

forward peaked than the measured values from [13, 17]. At 30 eV our result compares well with the experimental data only for larger angles. The good agreement between measured DCS and the results obtained in the four-state calculations from Parker *et al* [25] (complex-Kohn) and Machado *et al* [28] (MCF) points out that the coupling among $b^3\Sigma_u^{(+)}$, $a^3\Sigma_g^{(+)}$ and $c^3\Pi_u^{(+)}$ triplet states, in the angular region from 15° to around 90°, would be very important. In figure 3(d) we see that, although strongly affected by the presence of resonant structures, our integral cross section is in very good agreement with available experimental data from [13, 14] and [17]. Accordance among ICS results obtained from distinct theoretical methods is quite reasonable for energies above 20 eV. Finally, we notice the appearance of a sharp resonance at 12.5 eV and we found that it is associated with configurations of the $\Sigma_u^{(+)}$ symmetry. It is important to note that the ICS result from Branchett *et al* [31] (*R*-matrix) also displays, around the energy of 12.9 eV, a less pronounced resonant structure.

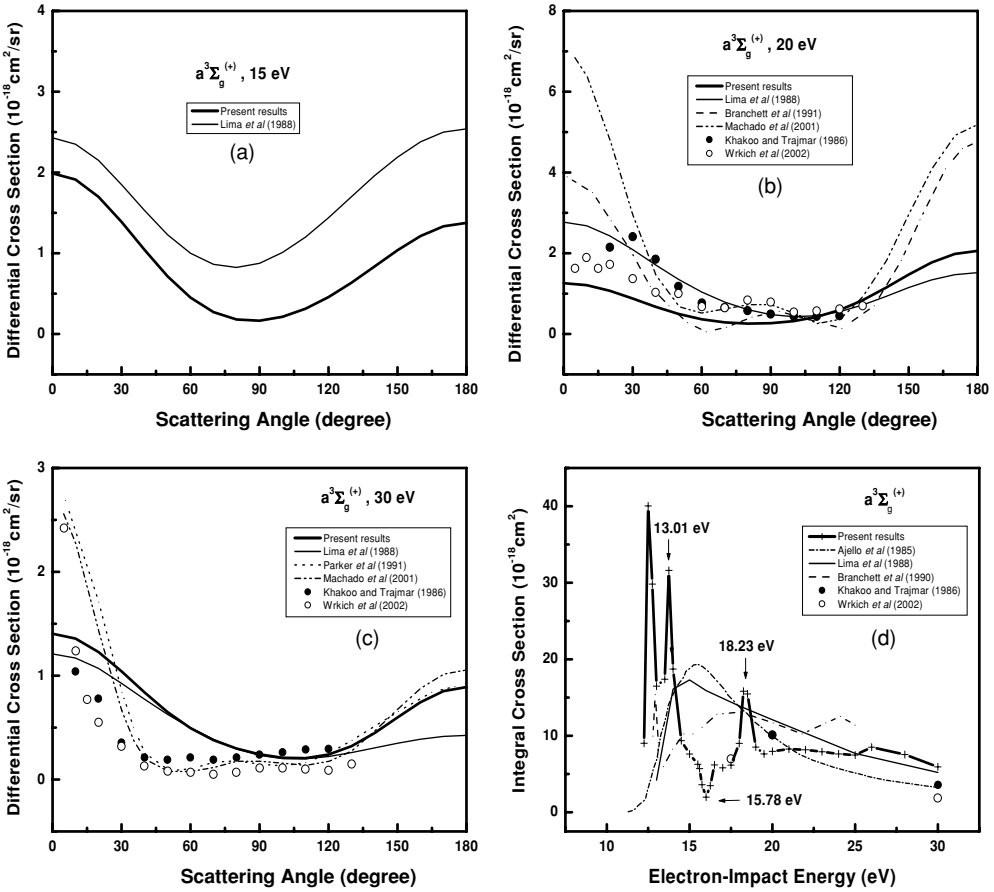

Figure 3. Differential and integral cross sections for the $X^1\Sigma_g^{(+)} \rightarrow a^3\Sigma_g^{(+)}$ electronic transition of the H_2 molecule: (a) DCS at 15 eV, (b) DCS at 20 eV, (c) DCS at 30 eV and (d) ICS. As in figure 1, except, short-dash-dotted line: Ajello *et al* [53]; dotted line: complex-Kohn four-state results from Parker *et al* [25]; open circles, experimental results from Wrkich *et al* [17].

3.3.4. The $X^1\Sigma_g^{(+)} \rightarrow E,F^1\Sigma_g^{(+)}$ electronic transition. Differential cross sections for the $X^1\Sigma_g^{(+)} \rightarrow E,F^1\Sigma_g^{(+)}$ electronic transition are presented in figures 4(a)–(c). At the incident energy of 15 eV the MOB-SCI result shows a relatively flat angular distribution and lies systematically below the DCS obtained with two-state (SMC) and four-state (MCF) [29] close-coupling calculations. At 20 eV, our result is also lower than those calculated by Branchett *et al* (*R*-matrix) [31] and Machado *et al* (MCF) [29], but compares very well with the measured values from Wrkich *et al* [17]. For the energy of 30 eV the agreement of our DCS with respect to other theoretical results and the experimental data from [17] is quite reasonable, especially in the angular region above 30°. For small scattering angles the MOB-SCI cross section is less forward peaked. As could be seen in figure 4(d), there is a general disagreement between calculated and measured ICSs for this electronic transition. Nevertheless, the MOB-SCI result is in excellent agreement with the measurements from Wrkich *et al* [17]. A sharp resonance, associated with configurations of the Π_u symmetry, is found at around 13.75 eV.

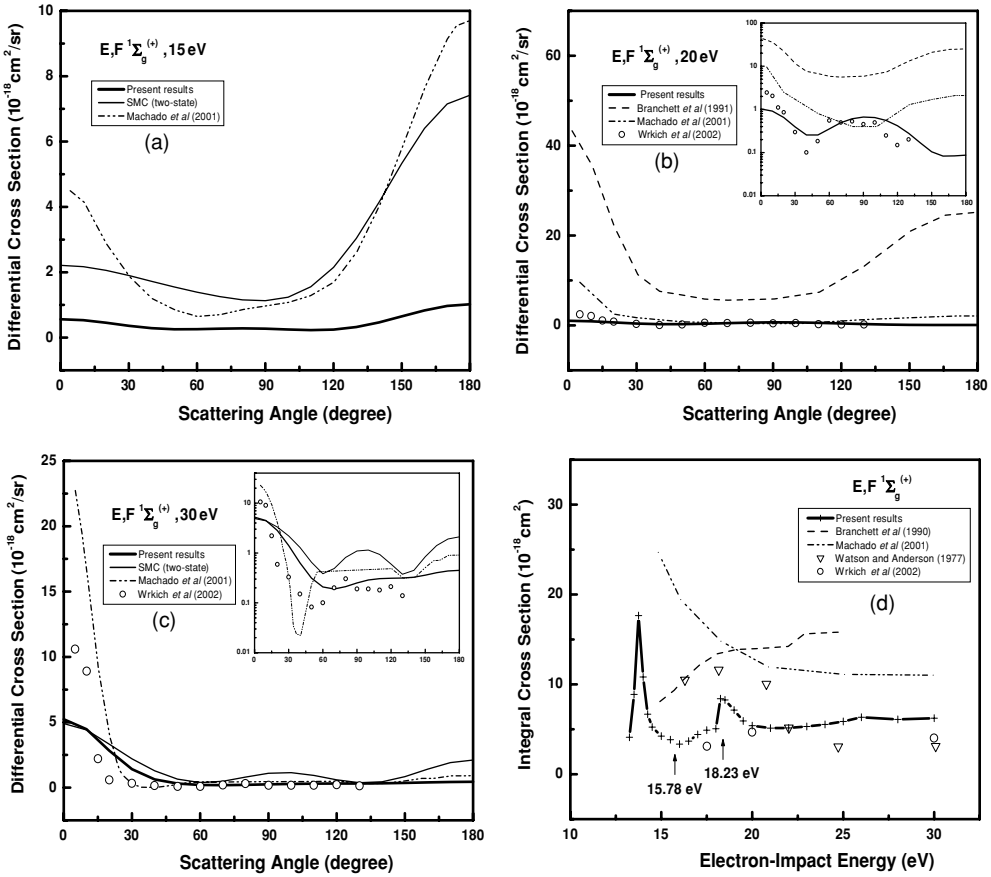

Figure 4. Differential and integral cross sections for the $X^1\Sigma_g^{(+)} \rightarrow E,F^1\Sigma_g^{(+)}$ electronic transition of the H_2 molecule: (a) DCS at 15 eV, (b) DCS at 20 eV, (c) DCS at 30 eV and (d) ICS. As in figure 2, except, solid line: SMC two-state results; down triangles: experimental results from Watson and Anderson [7].

3.3.5. The $X^1\Sigma_g^{(+)} \rightarrow c^3\Pi_u$ electronic transition. The DCS results presented in figures 5(a)–(c) correspond to the electronic transition between the ground and degenerated $c^3\Pi_u$ states. Firstly we note that, for all considered energies and in the whole angular region, the magnitude of the cross sections obtained by the nine-state MOB-SCI calculation is significantly smaller than previous SMC two-state results from Lima *et al* [22]. The agreement with the experimental data from [14, 17] is quite good, except at 20 eV for the angles below 90°. In particular, we note that at this energy the DCS results obtained by the four-state complex-Kohn [25] and the seven-state *R*-matrix [32] calculations are better compared with the measurements from Wrkich *et al* [17]. It may indicate that at this energy the coupling effects between states which are not included in our MOB-SCI calculation would be important. The integral cross section (ICS) shown in figure 5(d) clearly mirrors the general features pointed out in the above discussion. That is, the MOB-SCI result is smaller in magnitude if compared with the ICS obtained by the SMC two-state calculation [22] and compares very well with the measured values from Khakoo and Trajmar [14] and Wrkich *et al* [17]. The agreement with the theoretical results from [32, 28] is fair, especially at higher energies.

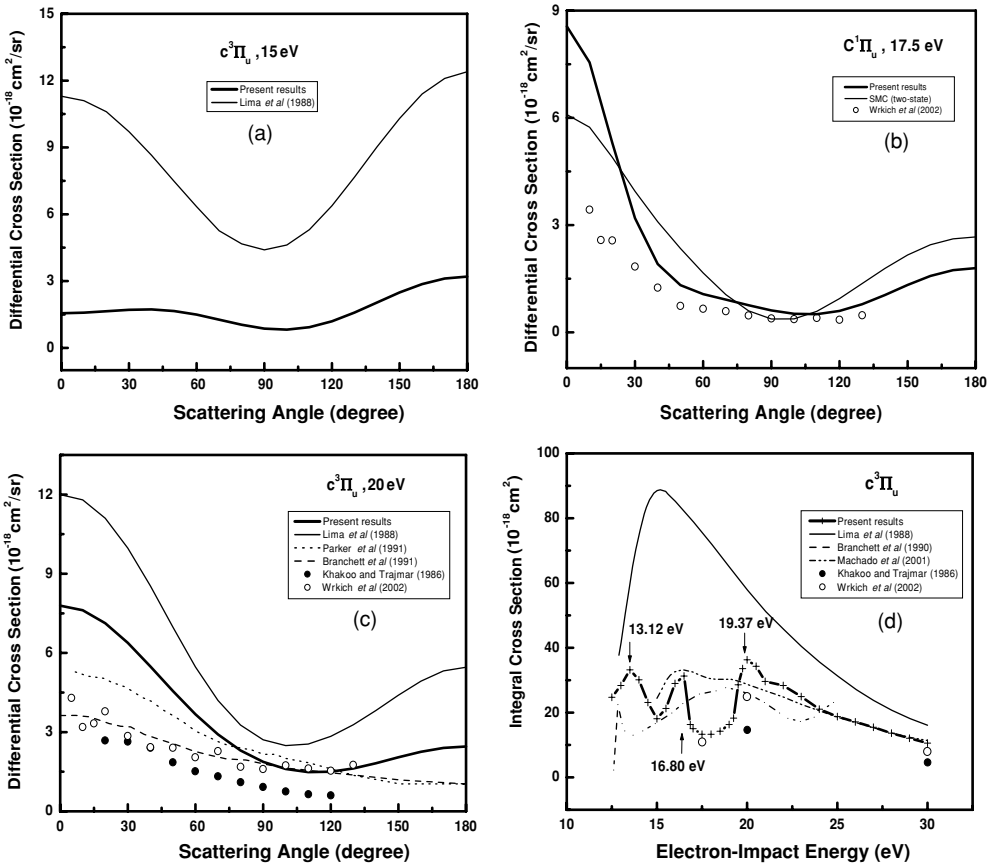

Figure 5. Differential and integral cross sections for the $X^1\Sigma_g^{(+)} \rightarrow c^3\Pi_u$ electronic transition of the H_2 molecule: (a) DCS at 15 eV, (b) DCS at 17.5 eV, (c) DCS at 20 eV and (d) ICS. As in figure 1, except, open circles: experimental results from Wrkich *et al* [17].

3.3.6. The $X^1\Sigma_g^{(+)} \rightarrow C^1\Pi_u$ electronic transition. In figures 6(a)–(c) we show the DCS results for the $X^1\Sigma_g^{(+)} \rightarrow C^1\Pi_u$ electronic transition at incident energies of 15, 17.5 and 20 eV. As it would be expected, this optically allowed transition provides very forward peaked differential cross sections. At 15 eV, we note that the DCS obtained by distinct theoretical approaches are quite different. The MOB-SCI result displays a nearly flat distribution for angles above 60° and is less forward peaked than the cross section obtained by the MCF four-state calculation from Machado *et al* [29]. Once again, the lack of experimental measurements at lower energies prevents a more elaborated discussion. For the energies of 17.5 and 20 eV, the MOB-SCI results are in better agreement with respect to the measured values from [14, 17] than those obtained by the SMC two-state calculation from Lima *et al* [22]. Finally, from figure 6(d) we note that the MOB-SCI integral cross section displays a reasonable agreement with the experimental data from Ajello *et al* [10] and Wrkich *et al* [17] and reproduces the energy dependence obtained by the four-state calculation from Machado *et al* [29] (MCF) in shape, but not in magnitude.

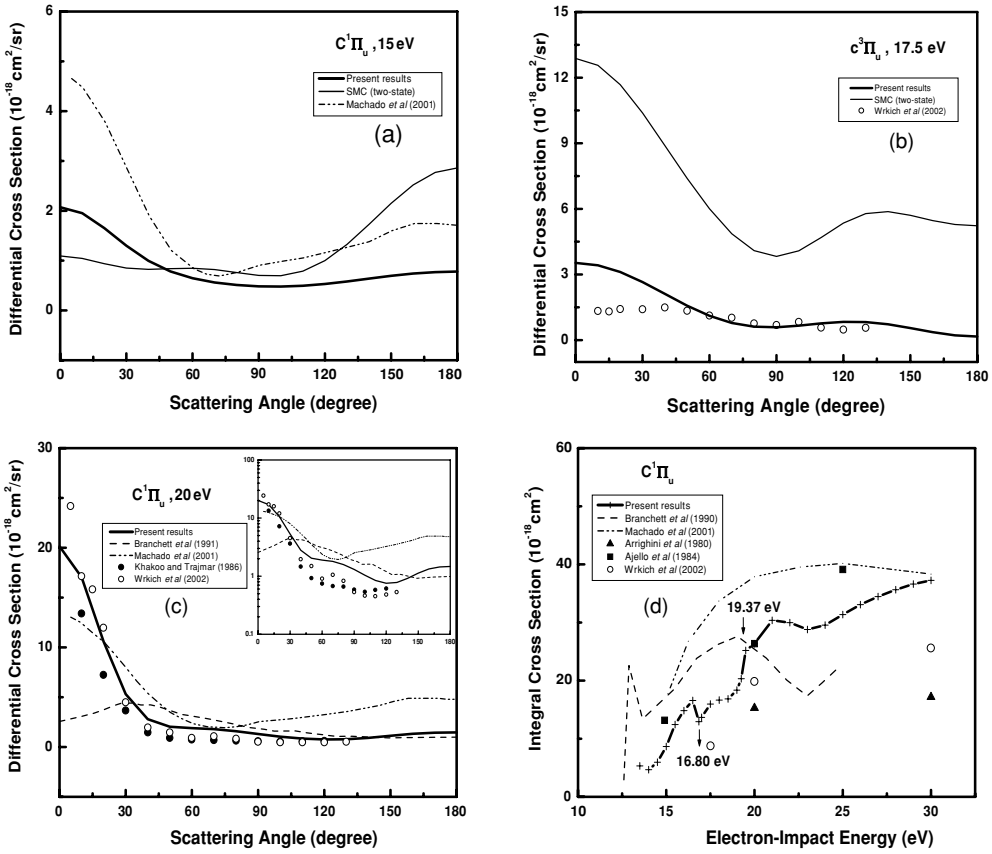

Figure 6. Differential and integral cross sections for the $X^1\Sigma_g^{(+)} \rightarrow C^1\Pi_u$ electronic transition of the H_2 molecule: (a) DCS at 15 eV, (b) DCS at 17.5 eV, (c) DCS at 20 eV and (d) ICS. As in figure 2, except, solid line: SMC two-state results; full triangles and full squares: results from Arrighini *et al* [52] and Ajello *et al* [10].

4. Summary and conclusions

In this paper, we have presented an application of the SMC method in the study of the electronic excitation of H_2 molecules by impact of low-energy electrons. The scattering amplitudes were obtained within the MOB-SCI level of approximation, giving rise to a five-state (nine, for degenerated Π_u states) close-coupling calculations.

Through the use of the MOB-SCI strategy we have observed a systematic reduction effect in the magnitude of the calculated cross section if compared with those obtained by earlier two-state calculations. The overall agreement between our results and the experimental data is, in general, quite good and emphasize the importance of inclusion of multichannel effects in the description of the excitation processes considered in this work. Besides, the coupling between singlet and triplet states of the same spatial symmetry shows to be very strong and it is a feature for the first time accounted in the study of e^-–H_2 electronic transitions.

In summary, this work highlights the advantages of the present strategy and represents a clear invitation for further investigations. In particular, we are interested to apply the MOB-SCI approach to studies of electron collisions with larger molecules, where the high density

of energetically accessible electronic target states makes the use of standard close-coupling models prohibitive.

Acknowledgments

RFC was supported by a graduate fellowship by FAPESP (Fundação para o Amparo à Pesquisa do Estado de São Paulo) and MAPL was supported by a grant by CNPq (Conselho Nacional de Desenvolvimento Científico e Tecnológico).

References

[1] Garscadden A 1992 *Z. Phys.* D **24** 97
[2] Huo W M and Kim Y K 1999 *IEEE Trans. Plasma Sci.* **27** 1225
[3] Christophorou L G and Olthoff J K 2002 *Appl. Surf. Sci.* **192** 309
[4] Brunger M J and Buckman S J 2002 *Phys. Rep.* **357** 215
[5] Trajmar S, Cartwright D C, Rice J K, Brinkmann R T and Kupperman A 1968 *J. Chem. Phys.* **49** 5464
[6] Weingartshofer A, Ehrhardt H, Hermann V and Linder F 1970 *Phys. Rev.* A **2** 294
[7] Watson J and Anderson R J 1977 *J. Chem. Phys.* **66** 4025
[8] Srivastava S K and Jensen S 1977 *J. Phys. B: At. Mol. Phys.* **10** 3341
[9] Hall R I and Andric L 1984 *J. Phys. B: At. Mol. Phys.* **17** 3815
[10] Ajello J M, Shemansky D, Kwok T L and Yung Y L 1984 *Phys. Rev.* A **29** 636
[11] Nishimura H and Danjo A 1986 *J. Phys. Soc. Japan* **55** 3031
[12] Mason N J and Newell W R 1986 *J. Phys. B: At. Mol. Opt. Phys.* **19** L203
[13] Khakoo M A and Trajmar S 1986 *Phys. Rev.* A **34** 138
[14] Khakoo M A and Trajmar S 1986 *Phys. Rev.* A **34** 146
[15] Khakoo M A, Trajmar S, McAdams R and Shyn T W 1987 *Phys. Rev.* A **35** 2832
[16] Khakoo M A and Segura J 1994 *J. Phys. B: At. Mol. Opt. Phys.* **27** 2355
[17] Wrkich J, Mathews D, Kanik I, Trajmar S and Khakoo M A 2002 *J. Phys. B: At. Mol. Opt. Phys.* **35** 4695
[18] Goddard W A III and Hunt W J 1974 *Chem. Phys. Lett.* **24** 464
[19] Baluja K L, Noble C J and Tennyson J 1985 *J. Phys. B: At. Mol. Phys.* **18** L851
[20] Schneider B I and Collins L 1985 *J. Phys. B: At. Mol. Phys.* **18** L857
[21] Lima M A P, Gibson T L, Huo W M and McKoy V 1985 *J. Phys. B: At. Mol. Phys.* **18** L865
[22] Lima M A P, Gibson T L, McKoy V and Huo W M 1988 *Phys. Rev.* A **38** 4527
[23] Gibson T L, Lima M A P, McKoy V and Huo W M 1987 *Phys. Rev.* A **35** 2473
[24] Rescigno T N and Schneider B I 1988 *J. Phys. B: At. Mol. Opt. Phys.* **21** L691
[25] Parker S D, McCurdy C W, Rescigno T N and Lengsfield B H III 1991 *Phys. Rev.* A **43** 3514
[26] Lee M T, Fujimoto M M, Kroin T and Iga I 1996 *J. Phys. B: At. Mol. Opt. Phys.* **29** L425
[27] Lee M T, Fujimoto M M and Iga I 1998 *J. Mol. Struc.* **432** 197
[28] Machado A M, Fujimoto M M, Taveira A M A, Brescansin L M and Lee M T 2001 *Phys. Rev.* A **63** 032707
[29] Machado A M, Taveira A M A, Brescansin L M and Lee M T 2001 *J. Mol. Struc.* **574** 133
[30] Branchett S E and Tennyson J 1990 *Phys. Rev. Lett.* **64** 2889
[31] Branchett S E, Tennyson J and Morgan L A 1990 *J. Phys. B: At. Mol. Opt. Phys.* **23** 4625
[32] Branchett S E, Tennyson J and Morgan L A 1991 *J. Phys. B: At. Mol. Opt. Phys.* **24** 3479
[33] Trevisan C S and Tennyson J 2001 *J. Phys. B: At. Mol. Opt. Phys.* **34** 2935
[34] da Costa R F, da Paixão F J and Lima M A P 2004 *J. Phys. B: At. Mol. Opt. Phys.* **37** L129
[35] Takatsuka K and McKoy V 1981 *Phys. Rev.* A **24** 2473
[36] Takatsuka K and McKoy V 1984 *Phys. Rev.* A **30** 1734
[37] Chaudhuri P, Varella M T N, Carvalho C R C and Lima M A P 2004 *Nucl. Instrum. Methods Phys. Res.* **221** 69
[38] Chaudhuri P, Varella M T N, Carvalho C R C and Lima M A P 2004 *Phys. Rev.* A **69** 042703
[39] Lippmann B A and Schwinger J 1950 *Phys. Rev.* **79** 469
[40] Lima M A P and McKoy V 1988 *Phys. Rev.* A **38** 501
[41] Lima M A P, Brescansin L M, da Silva A J R, Winstead C and McKoy V 1990 *Phys. Rev.* A **41** 327
[42] Lima M A P, Gibson T L, Takatsuka K and McKoy V 1984 *Phys. Rev.* A **30** 1741
[43] Lane N F 1980 *Rev. Mod. Phys.* **52** 29
[44] Kolos W and Roothaan C C J 1960 *Rev. Mod. Phys.* **32** 219
[45] Kolos W and Wolniewicz L 1965 *J. Chem. Phys.* **43** 2429

[46] Kolos W and Wolniewicz L 1968 *J. Chem. Phys.* **48** 3672
[47] Kolos W and Rychlewski J 1977 *J. Mol. Spectrosc.* **66** 428
[48] Kolos W and Dresser K 1985 *J. Chem. Phys.* **82** 3292
[49] Rothenberg S and Davidson E R 1966 *J. Chem. Phys.* **44** 730
[50] Sharp T E 1971 *At. Data* **2** 119
[51] Winstead C and McKoy V 1990 *Phys. Rev.* A **41** 49
[52] Arrighini G P, Biondi F and Guidotti C 1980 *Mol. Phys.* **41** 1501
[53] Ajello J M, Pang K D, Franklin B and Fram F 1985 *EOS Trans. Am. Geophys. Union* **66** 989